Eur. Phys. J. C 49, 559–567 (2007)
DOI 10.1140/epjc/s10052-006-0153-y

THE EUROPEAN PHYSICAL JOURNAL C

Regular Article – Experimental Physics

ψ' production in Pb–Pb collisions at 158 GeV/nucleon

The NA50 Collaboration

B. Alessandro[10], C. Alexa[3], R. Arnaldi[10], M. Atayan[12], S. Beolè[10], V. Boldea[3], P. Bordalo[6,a], G. Borges[6], J. Castor[2], B. Chaurand[9], B. Cheynis[11], E. Chiavassa[10], C. Cicalò[4], M.P. Comets[8], S. Constantinescu[3], P. Cortese[1], A. De Falco[4], N. De Marco[10], G. Dellacasa[1], A. Devaux[2], S. Dita[3], O. Drapier[9], J. Fargeix[2], P. Force[2], M. Gallio[10], C. Gerschel[8], P. Giubellino[10], M.B. Golubeva[7], M. Gonin[9], A. Grigoryan[12], J.Y. Grossiord[11], F.F. Guber[7], A. Guichard[11], H. Gulkanyan[12], M. Idzik[10,b], D. Jouan[8], T.L. Karavicheva[7], L. Kluberg[9], A.B. Kurepin[7], Y. Le Bornec[8], C. Lourenço[5], M. Mac Cormick[8], A. Marzari-Chiesa[10], M. Masera[10], A. Masoni[4], M. Monteno[10], A. Musso[10], P. Petiau[9], A. Piccotti[10], J.R. Pizzi[11,c], F. Prino[10], G. Puddu[4], C. Quintans[6], L. Ramello[1], S. Ramos[6,a], L. Riccati[10], A. Romana[9,c], H. Santos[6,d], P. Saturnini[2], E. Scomparin[10], S. Serci[4], R. Shahoyan[6,e], M. Sitta[1], P. Sonderegger[5,a], X. Tarrago[8], N.S. Topilskaya[7], G.L. Usai[4], E. Vercellin[10], L. Villatte[8], N. Willis[8]

[1] Universitá del Piemonte Orientale, Alessandria and INFN-Torino, Italy
[2] LPC, Univ. Blaise Pascal and CNRS-IN2P3, Aubière, France
[3] IFA, Bucharest, Romania
[4] Università di Cagliari/INFN, Cagliari, Italy
[5] CERN, Geneva, Switzerland
[6] LIP, Lisbon, Portugal
[7] INR, Moscow, Russia
[8] IPN, Univ. de Paris-Sud and CNRS-IN2P3, Orsay, France
[9] LLR, Ecole Polytechnique and CNRS-IN2P3, Palaiseau, France
[10] Università di Torino/INFN, Torino, Italy
[11] IPN, Univ. Claude Bernard Lyon-I and CNRS-IN2P3, Villeurbanne, France
[12] YerPhI, Yerevan, Armenia

Dedicated to the memory of our colleagues Albert Romana and Jean René Pizzi, whose untimely death occurred while finalizing this article.

Received: 22 May 2006 / Revised version: 25 September 2006 /
Published online: 21 November 2006 –

Abstract. ψ' production is studied in Pb–Pb collisions at 158 GeV/c per nucleon incident momentum. Absolute cross-sections are measured and production rates are investigated as a function of the centrality of the collision. The results are compared with those obtained for lighter colliding systems and also for the J/ψ meson produced under identical conditions.

PACS. 25.75.Dw

1 Introduction

The production of charmonium states in ultrarelativistic heavy ion collisions has been investigated since the mid 80s by the NA38 Collaboration [1], followed in the 90s by NA50 [2]. The motivation is to search for the phase transition of nuclear matter from its normal state to a deconfined quark-gluon plasma, as predicted to occur, under extreme energy densities or temperatures, by non-perturbative QCD. In such a deconfined matter, charmonia states, in particular the J/ψ vector-meson, have been predicted to be suppressed by Debye colour screening [3]. Indeed, the NA50 experiment has shown that J/ψ production in Pb–Pb collisions is significantly suppressed with respect to the expectations derived from the rates measured in proton, oxygen and sulphur-induced reactions [4–6]. The ψ' is a more loosely bound state than the J/ψ, which opens the possibility that it may dissociate at lower energy densities in connection with critical scenarios, as predicted by recent lattice calculations [7, 8], but also be sensi-

[a] also at IST, Universidade Técnica de Lisboa, Lisbon, Portugal
[b] also at Faculty of Physics and Nuclear Techniques, AGH University of Science and Technology, Cracow, Poland
[c] deceased
[d] email: helena@lip.pt
[e] on leave of absence of YerPhI, Yerevan, Armenia

tive to other mechanisms, as absorption in nuclear matter or dissociation by co-moving hadrons. After the first results on ψ' production obtained by experiments NA38 [9] and NA50 [10], the framework for a general understanding of charmonium dissociation due to critical transitions has recently opened up with new experimental results on J/ψ suppression [11, 12]. The measurement of ψ' production reported hereafter, performed with identical analysis procedures as for the J/ψ, should help and internally constrain the various theoretical approaches which try to give a coherent overall picture of charmonium production and suppression.

2 Experimental setup, data selection and analysis method

NA50 is a fixed target experiment at the CERN-SPS optimized for the detection of muon pairs produced in nucleus-nucleus collisions. The main component of the apparatus is a muon spectrometer made of an air-core toroidal magnet surrounded by two sets of multi-wire proportional chambers and trigger hodoscopes. An appropriate hadron absorber separates the spectrometer from the target itself, allowing the experiment to run with a high intensity incident beam and a moderate spectrometer illumination. Three independent detectors, located immediately downstream from the target region, measure the centrality of the reactions – a silicon strip multiplicity detector sampling the produced secondary charged particles, a Pb-scintillating fibers electromagnetic calorimeter measuring the neutral transverse energy $E_{\rm T}$ and a very forward hadronic calorimeter (zero degree calorimeter), embedded in the hadron absorber, which essentially measures the energy of the beam spectator nucleons in the collision, $E_{\rm ZDC}$. A beam hodoscope (BH), located 25 m upstream from the target, allows to monitor and identify the incident beam and also provides an accurate time reference for trigger purposes. A detailed description of the NA50 apparatus can be found in [13].

This article is based only on the highest quality data samples collected by the experiment in years 1998 and 2000 when only one single target was used which, moreover, was placed in vacuum in year 2000. These features have efficiently solved problems affecting previous data collections such as secondary fragment reinteractions within the target assembly leading to a centrality smearing on one hand and Pb–air interactions simulating peripheral Pb–Pb collisions on the other. Furthermore, the selected data have benefited from an upgraded track reconstruction treatment based on improved software algorithms [5, 14]. The data were collected with a typical beam intensity of $1\text{–}1.4 \times 10^7$ ions/s, over 4.8 s bursts every 20 s, at 158 GeV per nucleon. The single Pb target was 4 mm thick in 2000 (3 mm in 1998), equivalent to 10% (7%) of an interaction length. Muon pairs are selected in the rapidity window $2.92 \leq y_{\rm lab} < 3.92$ ($0 \leq y_{\rm CM} < 1$) and with a Collins–Soper angle $|\cos\theta_{\rm CS}| < 0.5$, resulting in an acceptance of around 14%. On-target interactions are selected requiring the proper correlation between hits in the two planes of the multiplicity detector. This target selection procedure is 88% efficient for $E_{\rm T} > 5$ GeV and 100% efficient for $E_{\rm T} > 22$ GeV. It allows to unambiguously identify the most peripheral on-target interactions and, therefore, has now been applied to the Pb–Pb data samples collected both in 1998 and in 2000. Moreover, muons produced off-target are further excluded by a cut on the transverse distance, in the middle target plane, between the muon track extrapolated from the spectrometer and the beam axis. Parasitic interactions occurring upstream from the target, mostly in the beam hodoscope, are rejected by a BH interaction detector and by anti-halo counters. Multiple piled-up interactions are discarded by a shape analysis of the signal from the electromagnetic calorimeter. Residual piled-up events are rejected by a 2σ cut in the $E_{\rm T} - E_{\rm ZDC}$ correlation [2].

The opposite-sign dimuon invariant mass spectrum in the mass region of interest, as shown in Fig. 1, results from five different contributions – the resonances J/ψ and ψ', as well as the continuum formed by Drell–Yan, by open charm semi-leptonic decays and by the *unphysical* combinatorial background originating mostly from uncorrelated π and K decays. In order to disentangle the different contributions and to provide the necessary ingredients for the determination of cross-sections, a Monte–Carlo simulation technique is used. It allows to determine both the acceptance of each physical process and the smearing of the corresponding detected muon pairs as they result from the actual experimental detector and selection criteria imposed on the data. Each physical process is separately generated and its corresponding muon pairs are propagated through the detector exactly the way real muons do, which accounts, in particular, for multiple scattering and energy loss in the absorbers

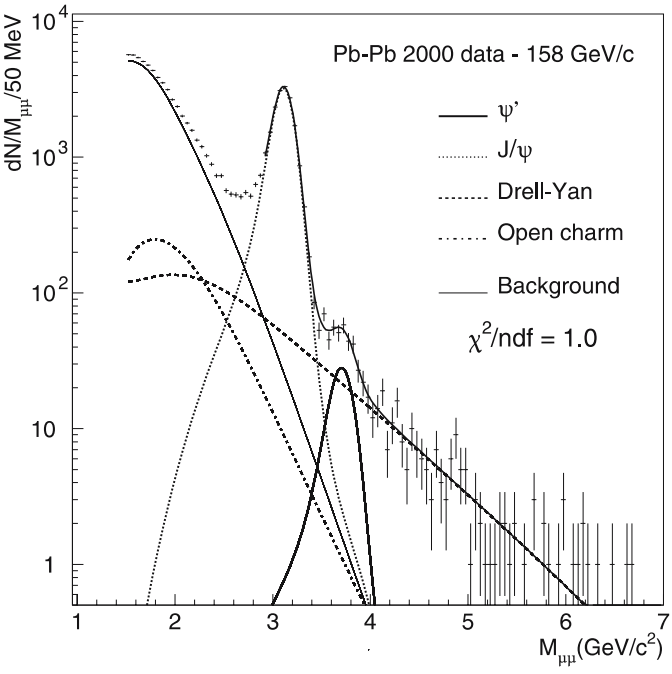

Fig. 1. The fitted opposite sign dimuon invariant mass spectrum, for mid-centrality Pb–Pb collisions

and for the limited acceptance of the apparatus. The resulting smearing is particularly visible in the J/ψ and ψ' reconstructed shapes, entirely due to the experimental resolution of the apparatus. The resonances are generated in rapidity with a Gaussian distribution of 0.6 units width. The transverse momentum used in the simulation follows the parametrization of a thermal distribution, $\mathrm{d}\sigma/\mathrm{d}p_\mathrm{T} = p_\mathrm{T} M_\mathrm{T} K_1(M_\mathrm{T}/T)$, where K_1 is the modified Bessel function of the second kind and first order, in the transverse mass, with $T = 236$ MeV. These parameters were tuned in order to reproduce the experimental spectra of the S–U collision system at 200 GeV/c [15] and they account very well for Pb–Pb interactions at 158 GeV/c [16]. The Drell–Yan is evaluated with PYTHIA [17], using the GRV LO 94 [18] set of parton density functions, with a minimum 4-momentum transfer and x domain as required by the NA50 phase space window. At the Born level, dimuons are produced with zero p_T; to overcome this inadequate physical picture, a primordial k_T inside the hadrons is considered, according to a gaussian with 0.8 GeV/c width. The $D\overline{D}$ mesons are also generated with PYTHIA, at leading order of QCD, using $m_\mathrm{c} = 1.35$ GeV/c^2 and a gaussian distributed k_T with 1.0 GeV/c width [19]. The combinatorial background, free from any simulation, is completely determined both in shape and in amplitude from the measured like-sign pair distributions according to $N^{+-}_\mathrm{BG} = 2\sqrt{N^{++}N^{--}}$. This method holds as long as the spectrometer acceptance does not depend on the muon charge, which is ensured by an appropriate selection of events.

After the Monte-Carlo determination of the muon pair mass shapes of each physical process, their corresponding amplitudes are obtained from a fit to the opposite sign dimuon invariant mass spectrum of the selected events. The background contribution, already established through the procedure explained above, is fixed. The $D\overline{D}$ contribution, although tiny in the mass range of relevance for the ψ' amplitude determination and, moreover, practically uncorrelated with it, is roughly estimated from a separate fit in the dimuon mass range 1.7–2.2 GeV/c^2. For this purpose, the corresponding Drell–Yan is deduced from the extrapolation of the muon pairs sampled above 4.2 GeV/c^2, a mass region where Drell–Yan is the only contribution and is, therefore, unambiguously determined. The ψ', J/ψ and the whole Drell–Yan amplitudes are obtained from a fit in the mass range 2.9–7.0 GeV/c^2, with both the combinatorial background and $D\overline{D}$ contributions fixed. The set of parameters which maximize the log-likelihood function is found by the MINUIT package [20], which also evaluates the function in the neighbourhood of the minimum, thus providing the parameter statistical uncertainties. One should notice the good χ^2 of the fit shown in Fig. 1. Details on the analysis method are given in [16].

3 Absolute cross-sections

The study of ψ' production in Pb–Pb collisions implies special care with the data treatment, in particular in what concerns the identification of systematic sources, since this resonance yields a weak signal due both to its small dimuon branching ratio ($B_{\mu^+\mu^-} = (7.3 \pm 0.8) \times 10^{-3}$ [21]) and to its large suppression with increasing centrality of the collision. Another challenge is the extraction of the ψ' signal itself from the several overlapping dimuon sources.

In order to measure absolute cross-sections, data collected in the year 2000 were selected under strict criteria with respect to the stability of the experimental conditions. After the data selection described in the previous section and after correcting for the target identification inefficiency, about 900ψ' are left for further analysis. This absolute number of events must still be corrected for various detector inefficiencies, selection cut losses and acceptances in the NA50 phase space window, as detailed in Table 1. The main systematical uncertainty contributing to the errors of the acceptance values is the generation model assumed. In particular, if a Fermi motion model of the nucleons inside the nucleus is taken into account, the spectrometer acceptance of the resonances changes by $\sim 1.5\%$. In the case of Drell–Yan, different parton density functions lead to a 4% difference in the acceptances.

Absolute cross-sections for ψ' and J/ψ in the dimuon channel, as well as for Drell–Yan in the mass windows of $2.9 \le M_{\mu\mu} < 4.5$ and $4.2 \le M_{\mu\mu} < 7.0$ GeV/c^2, are displayed in Table 2 within the kinematical ranges defined in Sect. 2. The ψ' absolute cross-section is affected by a systematic uncertainty of 7%, obtained as the quadratic sum of all uncertainties considered, namely the errors on the absolute normalizations, fit method, spectrometer acceptances and uncertainties associated with the Monte-Carlo inputs, like parton density functions and c-quark mass. The latter, although directly related to Drell–Yan and open charm theoretical uncertainties, indirectly influence the ψ' fitted normalization. The main contributions to the uncertainty in the ψ' yield are the luminosity calculation, 4%, and the chosen PDFs to generate Drell–

Table 1. Detector efficiencies, selection cut losses and integrated acceptances

Detector efficiencies (%)	
Dimuon trigger	87 ± 1
Muon track reconstruction	94 ± 1
Beam hodoscope	83 ± 1
Lifetime of DAQ	96 ± 1
Target identification ($5 < E_\mathrm{T} < 22$ GeV)	87 ± 2
($E_\mathrm{T} > 22$ GeV)	≈ 100
Selection cut losses (%)	
Interaction pile-up	15.8 ± 1
$E_\mathrm{T} - E_\mathrm{ZDC}$ correlation	16.3 ± 1
BH interaction	2.2 ± 0.5
Acceptances (%)	
ψ'	14.8 ± 0.3
J/ψ	12.5 ± 0.2
Drell–Yan ($2.9 < M_{\mu\mu} < 4.5$)	13.8 ± 0.2
Drell–Yan ($4.2 < M_{\mu\mu} < 7.0$)	17.8 ± 0.7

Table 2. Inclusive cross-sections for ψ' and J/ψ, multiplied by their branching ratios into $\mu^+\mu^-$, and for Drell–Yan, in the 4.2–7.0 GeV/c^2 mass range

Cross-sections (μb) **in** $0 \leq y_{\rm CM} < 1$ **and** $\mid \cos\theta_{\rm CS} \mid < 0.5$
Pb+Pb $\rightarrow \psi' + X = 0.136 \pm 0.013^{+0.010}_{-0.006}$
Pb+Pb $\rightarrow J/\psi + X = 23.32 \pm 0.16 \pm 0.84$
Pb+Pb $\rightarrow$ Drell–Yan $(2.9 < M_{\mu\mu} < 4.5) + X = 1.37 \pm 0.07 \pm 0.05$
Pb+Pb $\rightarrow$ Drell–Yan $(4.2 < M_{\mu\mu} < 7.0) + X = 0.172 \pm 0.009 \pm 0.009$

Yan, 5.8%, estimated as the numerical change in the result when using CTEQ4L [22] instead of GRVLO94. On the other hand, it has been verified that the more recent GRVLO98 [23] induces a variation of less than 1.5% on the cross-section measurement. The systematic uncertainty due to the fit method is 2.8%. The J/ψ cross-section obtained here, $23.32 \pm 0.16 \pm 0.84\,\mu$b, is 6.5% higher than the one derived from the Pb–Pb data collected in year 1995, $21.9 \pm 0.2 \pm 1.6$ mub, reported in [13]. The difference results from the cumulative effects of the new J/ψ experimental line shape [14] and the higher number of tracks reconstructed. Although the better description of the resonance tails would lead to a 3.5% smaller cross-section, the new offline software algorithms [5] deal much better with the high MWPC occupancy levels induced by the Pb–Pb interactions and result in a net *increase* of the final cross-section value.

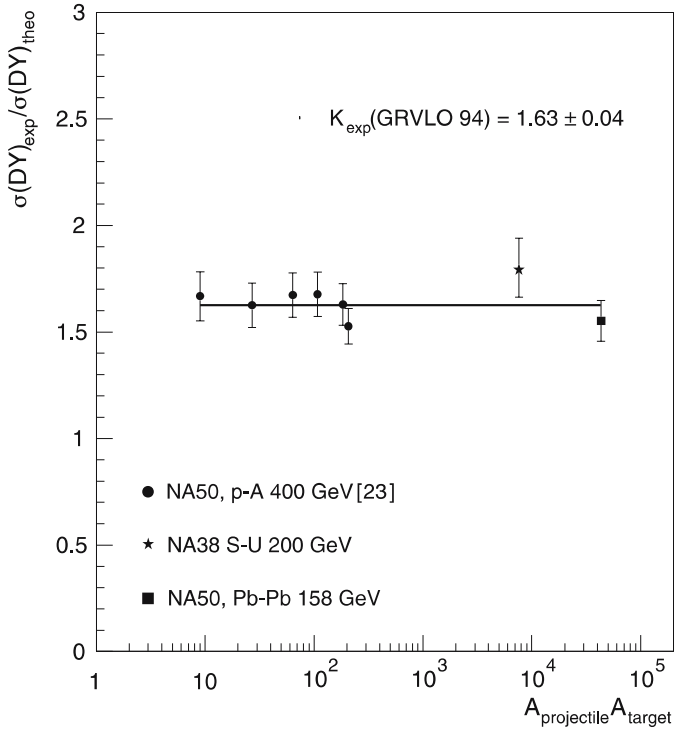

Fig. 2. The Drell–Yan $K_{\rm exp}$ factor measured at 158–400 GeV/c beam momenta in p–A and A–B collisions. GRV LO94 PDFs are used in the theoretical calculations and in the extraction of the measured values

Figure 2 shows the $K_{\rm exp}$ factor, the ratio between the measured Drell–Yan cross-section and the lowest order theoretical Drell–Yan cross-section. The constant behaviour of this ratio from p–Be to Pb–Pb collisions shows that the Drell–Yan process is proportional to the number of nucleon–nucleon collisions in the NA38/NA50 phase space window.

4 Cross-section ratios versus centrality

The study of the ψ' suppression as a function of centrality is based on 380 and 905ψ' events collected in 1998 and 2000, respectively, and analyzed as a function of their transverse energy used as the centrality estimator. Preliminary results of these studies have already been presented in [10].

For each centrality class separately, the analysis is performed as described in Sect. 2. In order to get the production pattern as a function of centrality, results in different classes have to be normalized with respect to each other. We have chosen to make use of the number of elementary nucleon-nucleon collisions for this normalization purpose and have replaced it by a proportional experimental direct estimate, namely the Drell–Yan cross-section in the corresponding centrality bin as determined from the same fit procedure. The method thus increases the robustness of the measured centrality pattern, as corrections and efficiencies depending on centrality, if any, cancel out in the ratio.

Figure 3 displays the ratio $B'_{\mu\mu}\sigma(\psi')/\sigma({\rm DY})$ as a function of the transverse energy, for the two data samples. We should note here that, although the target region was not in vaccum during the 1998 data taking period, the use of the multiplicity detector to tag in-target interactions has now allowed the study of peripheral collisions without ambiguities and, moreover, the results obtained from the year 1998 data sample are perfectly consistent with those obtained from the data collected in year 2000, when the target was in vacuum [16]. Thus, the 1998 data have been rebinned to match the same 2000 centrality intervals in order to perform their weighted average. The combined result shows a suppression of the ψ' production rate which becomes stronger with increasing centrality, up to a factor of 6 between peripheral and central collisions. Numerical values are reported in Table 3. Statistical and systematic errors have been quadratically added.

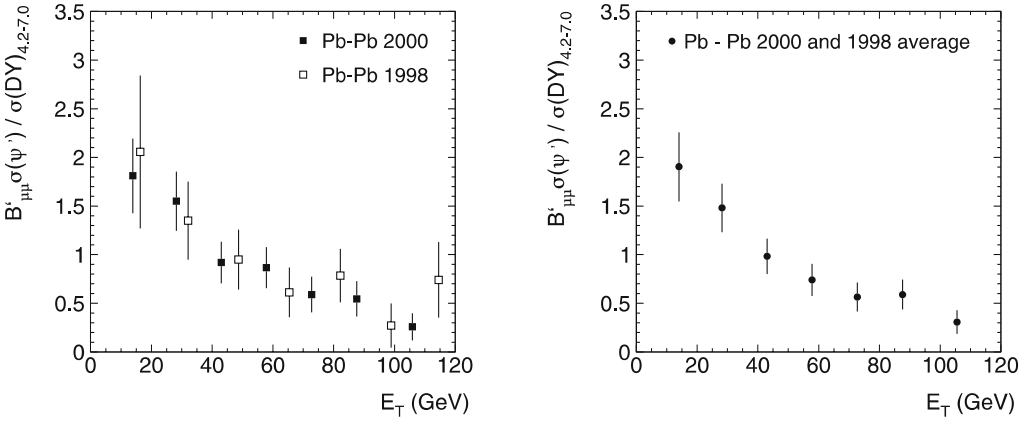

Fig. 3. $B'_{\mu\mu}\sigma(\psi')/\sigma(\mathrm{DY})$ as a function of E_T for the Pb–Pb 1998 and 2000 data samples (*left*). The cross-section ratios after combining the results obtained separately (*right*). Errors are the quadratic sum of statistical and systematic uncertainties

Table 3. $B'_{\mu\mu}\sigma(\psi')/\mathrm{DY}_{4.2-7.0}$ and $B'_{\mu\mu}\sigma(\psi')/B_{\mu\mu}\sigma(J/\psi)$ values for each centrality bin, for the weighted average between the 2000 and 1998 results. The first error is statistical, the second systematic

E_T range (GeV)	$\langle E_\mathrm{T}\rangle$ (GeV)	$B'_{\mu\mu}\sigma(\psi')/\sigma(\mathrm{DY}_{4.2-7.0})$	$B'_{\mu\mu}\sigma(\psi')/B_{\mu\mu}\sigma(J/\psi)\times 10^3$
3– 20	13.9	$1.91\pm0.35^{+0.03}_{-0.06}$	$9.30\pm1.24^{+0.28}_{-0.21}$
20– 35	28.2	$1.48\pm0.25^{+0.03}_{-0.04}$	$8.10\pm1.32^{+0.30}_{-0.19}$
35– 50	43.0	$0.98\pm0.18^{+0.02}_{-0.02}$	$7.33\pm1.35^{+0.35}_{-0.17}$
50– 65	57.8	$0.74\pm0.17^{+0.02}_{-0.01}$	$5.48\pm1.36^{+0.31}_{-0.13}$
65– 80	72.7	$0.56\pm0.15^{+0.01}_{-0.01}$	$4.77\pm1.40^{+0.32}_{-0.11}$
80– 95	87.6	$0.59\pm0.15^{+0.02}_{-0.01}$	$5.59\pm1.53^{+0.43}_{-0.12}$
95–150	105.9	$0.31\pm0.12^{+0.01}_{-0.01}$	$3.56\pm1.52^{+0.32}_{-0.08}$

PDF's used to generate Drell–Yan in the Monte Carlo simulations are the main contribution to the systematic errors, as explained in Sect. 3. They are centrality dependent, but small when compared with the statistical errors. The Drell–Yan mass range chosen to normalize the ψ' yield is 4.2–7.0 GeV/c^2. One can scale up the results to the mass range used in the J/ψ suppression studies, 2.9–4.5 GeV/c^2 [2], applying the factor 7.96, which is the ratio between the Drell–Yan cross-sections in the two mass domains (see Table 2).

The direct comparison between J/ψ and ψ' suppressions as a function of centrality is displayed on Fig. 4, which shows the ratio of cross-sections $B'_{\mu\mu}\sigma(\psi')/B_{\mu\mu}\sigma(J/\psi)$ as a function of transverse energy. The corresponding numerical values are reported in Table 3. The statistical errors come mainly from the ψ', since the J/ψ statistical uncertainty is less than 1%. Statistical and systematic errors have been added quadratically. From the steady decrease pattern of this ratio, we conclude that with respect to the J/ψ, the ψ' is more and more suppressed with increasing centrality, with a factor 2.5 between peripheral and central reactions.

Table 4 reports the number of ψ', J/ψ and Drell–Yan fitted events in each transverse energy interval. The numbers refer to both Pb–Pb 1998 and 2000 data taking periods.

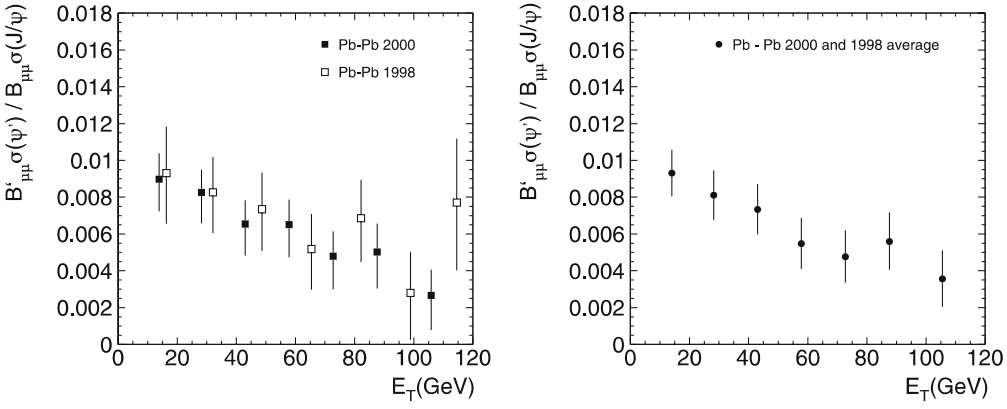

Fig. 4. $B'_{\mu\mu}\sigma(\psi')/B_{\mu\mu}\sigma(J/\psi)$ as a function of E_T for the Pb–Pb 1998 and 2000 data samples, separately for each year (*left*) and after combining both data sets (*right*). Errors are the quadratic sum of statistical and systematic uncertainties

Table 4. The numbers of ψ', J/ψ and $\mathrm{DY}_{4.2-7.0}$ fitted events for each centrality range. Errors are only statistical

E_{T} range (GeV)	ψ'	J/ψ	$\mathrm{DY}_{4.2-7.0}$
3– 20	186 ± 25	$16\,942 \pm 146$	112 ± 8
20– 35	243 ± 31	$25\,229 \pm 181$	187 ± 11
35– 50	227 ± 35	$27\,276 \pm 192$	264 ± 12
50– 65	193 ± 36	$27\,681 \pm 196$	288 ± 13
65– 80	154 ± 36	$27\,315 \pm 200$	310 ± 14
80– 95	159 ± 37	$25\,111 \pm 193$	311 ± 14
95–150	110 ± 40	$28\,570 \pm 209$	401 ± 15

5 Comparison with ψ' production in lighter collision systems

ψ' suppression in Pb–Pb collisions can be compared with results obtained both from NA50 proton-induced and NA38 S–U reactions, the latter reanalysed by the NA50 collaboration [24]. Data were collected with incident momentum beams of 400 and 450 GeV/c for protons and of 200 AGeV/c for sulphur ions. In the framework of NA50, a coherent comparison can be done, since these data were collected with the same spectrometer, so that systematic effects related to trigger and reconstruction efficiencies are similar for all data sets. Besides, the transverse energy released in S-U collisions has been measured with a very similar electromagnetic calorimeter. Correction factors have been applied to scale down the p–A and S–U center of mass energies and rapidity domains to the Pb–Pb conditions [25]. Taking into account the relative amount of protons and neutrons in each colliding nucleus, isospin corrections are needed when the Drell–Yan cross-section is compared among different systems. For this reason the measured Drell–Yan cross-sections have been normalized to proton–proton collisions. One should notice that, since ψ' production in the NA38/NA50 x_{F} domain is dominated by gluon fusion, rather than by quark–antiquark annihilation, the ψ' isospin corrections are negligible.

In order to compare the ψ' behaviour between different colliding systems we consider hereafter three variables directly related to the impact parameter of the interactions, namely L, the average path crossed by the $c\bar{c}$ pair inside the nucleus, N_{part}, the number of nucleons participating in the interaction, and ϵ, the reached energy density. They have been calculated through the Glauber model formalism [26] of nucleus–nucleus collisions. Such a model considers an A–B interaction as a superposition of independent interactions between the beam and target nucleons. The model also assumes that the nucleon–nucleon cross section remains unchanged as the two nuclei cross each other. One should bear in mind that this is an approximation because a nucleon, after a collision, may become excited and subsequently interact with other nucleon with a different cross section. The Pb nuclear density is parameterised by a two-parameters Fermi function [27], also known as the Woods–Saxon distribution, $\rho(r) = \rho_0/(1 + \exp((r - r_0)/c))$, where ρ_0 is the average nuclear density, taken as 0.17 fm^{-3}, r_0 is the half-density radius of 6.624 fm and c is a diffuseness parameter of 0.549 fm for protons. Taken into account the "neutron halo" effect [6, 28] a different diffuseness parameter (0.667 fm) is used to describe the neutrons distribution inside the Pb nucleus. The same model has been applied to the U nucleus, with a half-density radius of 6.8054 fm and diffuseness parameters of 0.605 fm for protons and 0.786 fm for neutrons. The actual shape of the U nucleus is not taken into account. Figure 5 shows the ratio $B'_{\mu\mu}\sigma(\psi')/\sigma(\mathrm{DY})$ as a function of L. The measured suppression patterns suggest the following three features: a) a fair agreement with exponential behaviours; b) two different regimes, one for proton and a different one for ion-induced reactions; c) a similar centrality dependence for S–U and Pb–Pb interations. Using an exponential parametrization to describe ψ' absorption as a function of L [29, 30], according to $\exp(-\langle\rho L\rangle\sigma_{\mathrm{abs}})$, the fit of the data gives an absorption cross-section of 7.3 ± 1.6 mb in p–A collisions, while a much higher value, 19.2 ± 2.4 mb, is obtained for ion–ion collisions (S–U and Pb–Pb fitted simultaneously). The left panel of Fig. 6 shows the same ratio as a function of the number of participants. By definition, a nucleon is designated as participant if it has at least one inelastic interaction with one or more surrounding nucleons. For this work the calculation of N_{part} has followed (9) of [31]. It is worth mentioning that, at SPS energies, several experiments have observed that the number of participating nucleons in a nucleus–nucleus collision scales with the transverse energy [32, 33]. The ψ' suppression as a function of the energy density is shown in the right panel of Fig. 6, but only for A–B collisions. In the framework of the Bjorken model [34], the energy density reached in a nucleus–nucleus collision is proportional to the number of participating nucleons per unit transverse area (see [16, 35] for examples of such an evaluation). An initial formation time, $\tau_0 = 1$ fm/c, has been assumed. It is important to keep in mind that the three centrality variables, L, N_{part} and ϵ, are strongly correlated, since they

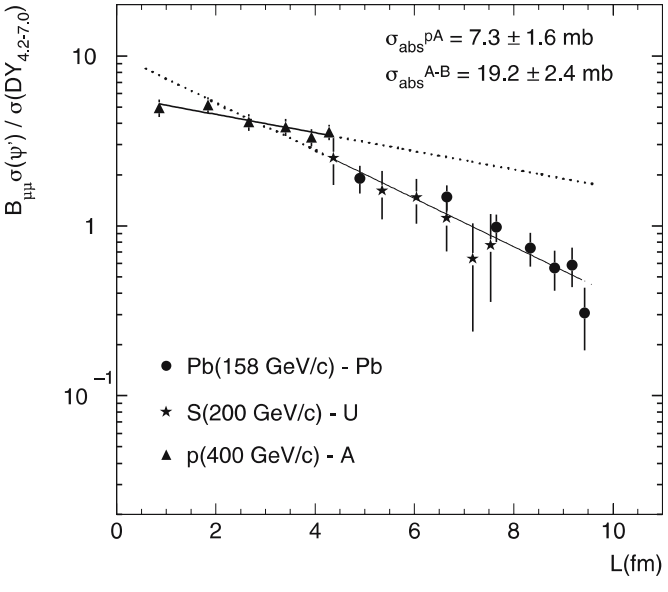

Fig. 5. $B'_{\mu\mu}\sigma(\psi')/\sigma(\mathrm{DY})$ as a function of L. Statistical and systematic uncertainties are added quadratically

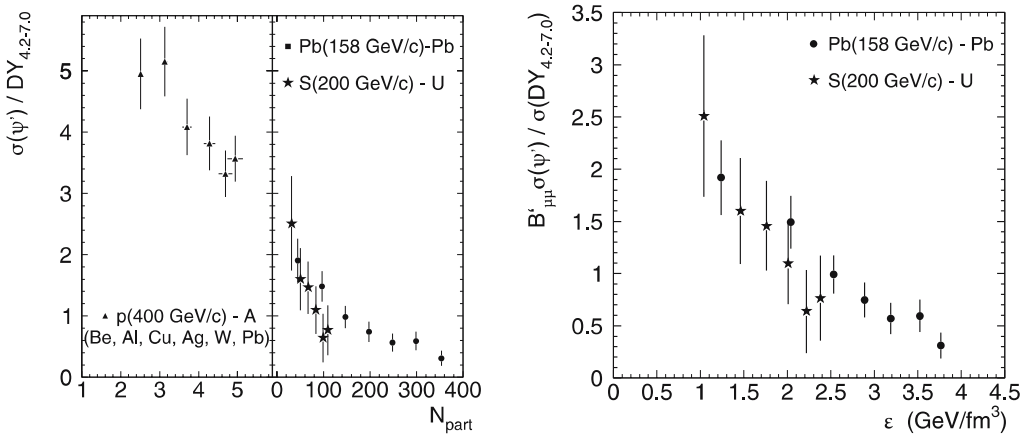

Fig. 6. $B'_{\mu\mu}\sigma(\psi')/\sigma(\mathrm{DY})$ as functions of the number of participating nucleons (*left*) and of the energy density (*right*). Statistical and systematic uncertainties are added quadratically

are all calculated by the same Glauber model of nucleus–nucleus collisions. Their average and r.m.s. values for each centrality bin are quoted in Tables 5 and 6, for Pb–Pb and S–U colliding systems, respectively. These values take into account the smearing due to the experimental resolution of the electromagnetic calorimeters used by NA50 and NA38. Concerning the energy density values, we are quite confident that the comparison between S–U and Pb–Pb is robust, while the absolute values could suffer from a 20%–25% systematic uncertainty.

In principle, the use of several centrality estimators in the study of the ψ' suppression pattern in two significantly different colliding systems, such as S–U and Pb–Pb, should indicate the centrality variable as a function of which the two measured suppression patterns would best overlap. In practice, however, the statistical errors of the ψ' suppression patterns presently available do not allow us to make very clear statements in this respect, apart from saying that the use of the N_{part} variable seems to result in a somewhat worse overlap between the two data sets. The Pb–Pb and S–U slopes, from a linear fit to the ψ'/DY ratio vs. N_{part} or ϵ in the overlapping centrality range, differ by 1.6 (resp. 1.0) standard deviations. These observations could also be slightly affected by the approximate nature of our calculations in what concerns the shape of the U nucleus, as mentioned before.

6 Comparison between J/ψ and ψ' suppressions

The ratio $B'_{\mu\mu}\sigma(\psi')/B_{\mu\mu}\sigma(J/\psi)$ as plotted in Fig. 7 shows the relative suppression of the two charmonium states as

Table 5. Mean free path crossed by the $c\bar{c}$ pair inside the nucleus, number of participating nucleons and energy densities for each Pb–Pb E_{T} range

E_{T} range (GeV)	$\langle E_{\mathrm{T}}\rangle$ (GeV)	$\langle L\rangle$ (fm)	r.m.s (fm)	$\langle N_{\mathrm{part}}\rangle$	r.m.s.	$\langle\epsilon\rangle$ (GeV/fm^3)	r.m.s. (GeV/fm^3)
3– 20	13.9	4.90	0.84	44.6	17.7	1.24	0.37
20– 35	28.2	6.65	0.44	96.7	18.0	2.04	0.20
35– 50	43.0	7.65	0.31	147.1	19.3	2.53	0.14
50– 65	57.8	8.34	0.24	197.7	20.6	2.89	0.11
65– 80	72.7	8.83	0.18	248.6	22.0	3.19	0.09
80– 95	87.6	9.17	0.14	299.2	23.0	3.52	0.07
95–150	105.9	9.43	0.10	353.3	22.4	3.76	0.06

Table 6. Same as previous table, for S–U collisions

E_{T} range (GeV)	$\langle E_{\mathrm{T}}\rangle$ (GeV)	$\langle L\rangle$ (fm)	r.m.s (fm)	$\langle N_{\mathrm{part}}\rangle$	r.m.s.	$\langle\epsilon\rangle$ (GeV/fm^3)	r.m.s. (GeV/fm^3)
13–28	22.1	4.37	0.54	31.3	9.1	1.04	0.22
28–40	34.3	5.35	0.43	50.0	9.7	1.46	0.18
40–52	46.3	6.04	0.41	66.7	10.8	1.76	0.16
52–64	58.3	6.65	0.41	83.5	11.7	2.01	0.15
64–76	70.2	7.17	0.38	98.8	11.0	2.22	0.13
76–88	81.7	7.53	0.29	109.0	8.2	2.38	0.09

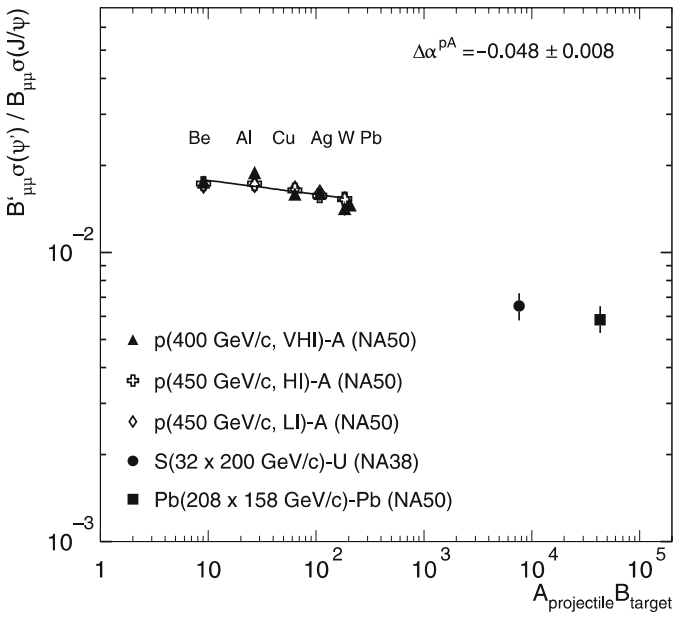

Fig. 7. $B'_{\mu\mu}\sigma(\psi')/B_{\mu\mu}\sigma(J/\psi)$ as a function of $A_{\rm projectile} \times B_{\rm target}$. Statistical and systematic uncertainties are added quadratically

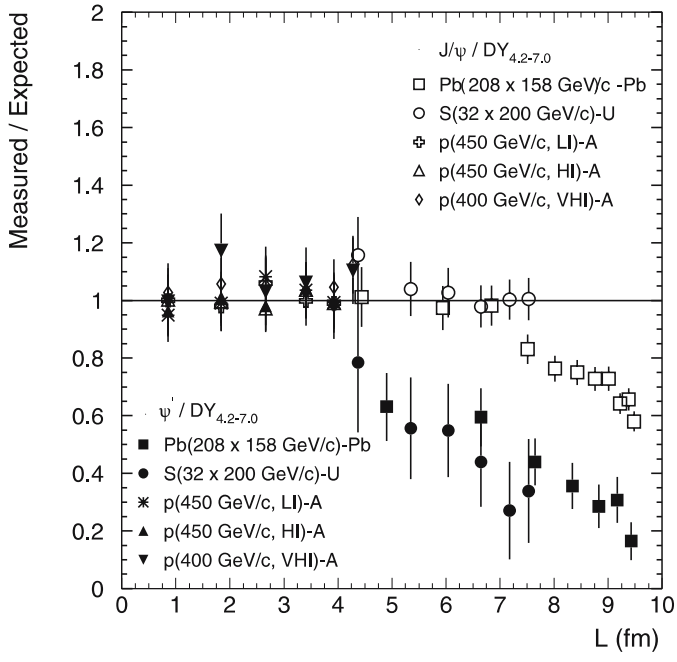

Fig. 8. The ratio "measured over expected" for the relative yields $B'_{\mu\mu}\sigma(\psi')/\sigma({\rm DY})$ and $B_{\mu\mu}\sigma(J/\psi)/\sigma({\rm DY})$, as a function of L

a function of the product of the projectile and target mass numbers. The ratio is parametrized, in the range of the p–A data points, by the power law $A^{\Delta\alpha}$, where α accounts for all nuclear effects suffered by the resonances. The measured negative value of this parameter, $\Delta\alpha = -0.048 \pm 0.008$, shows that the ψ' is more absorbed than the J/ψ, already in p–A collisions [5]. Furthermore, a strong suppression of the ψ' with respect to the J/ψ is measured for the ion induced reactions, S–U and Pb–Pb.

Figure 8 shows, for various interacting systems, the ratio between the measured charmonium yields, normalized to Drell–Yan dimuons, and the corresponding expected "normal nuclear absorptions". The latter are computed from the p–A results. Using full Glauber calculations, the absorption cross-sections in nuclear matter are $\sigma_{\rm abs}^{\rm Glb}(J/\psi) = 4.2 \pm 0.5\,{\rm mb}$ and $\sigma_{\rm abs}^{\rm Glb}(\psi') = 7.7 \pm 0.9\,{\rm mb}$, respectively [6, 24]. One should notice the good compatibility between this $\sigma_{\rm abs}^{\rm Glb}(\psi')$ value and the one obtained with a simple exponential in L, $7.3 \pm 1.6\,{\rm mb}$, as reported in Sect. 5. The figure shows that the departure from ordinary nuclear absorption occurs at a lower value of L for ψ' than for J/ψ. Moreover, while the ψ'/DY behaviour changes between p–A and the whole centrality range of ion-ion interactions, the J/ψ/DY trend in Pb–Pb collisions begins to be compatible with both p–A and S–U results, but deviates more and more as the collision centrality increases. More details on the J/ψ anomalous suppression in Pb–Pb interactions can be found in [2].

7 Conclusions

We have measured the ψ' absolute cross-section in Pb–Pb collisions at $\sqrt{s} = 17.3\,{\rm GeV}$, in the NA50 kinematic domain, $B'_{\mu\mu}\sigma(\psi') = 0.136 \pm 0.013({\rm stat}) + 0.010 - 0.006({\rm syst})$ μb. The study of the ψ' production as a function of centrality shows a steady decrease from peripheral to central collisions. It leads to a ψ' suppression factor of 6 relative to Drell–Yan production and of 2.5 relative to J/ψ. The comparison with lighter systems shows that the ψ' is much more suppressed in nucleus–nucleus than in proton–nucleus reactions and that the suppression pattern in S–U and Pb–Pb approximately overlap when studied as a function of L or energy density, while the overlap as a function of the number of participating nucleons seems to be somewhat worse. The comparison between the J/ψ and ψ' suppression patterns shows that the ψ' anomalous suppression sets in for lower values of L.

Acknowledgements. This work was partially supported by Fundação para a Ciência e a Tecnologia, Portugal.

References

1. NA38 Collaboration, M.C. Abreu et al., Eur. Phys. J. C **14**, 443 (2000) and references therein
2. NA50 Collaboration, B. Alessandro et al., Eur. Phys. J. C **39**, 335 (2005) and references therein
3. T. Matsui, H. Satz, Phys. Lett. B **178**, 416 (1986)
4. NA50 Collaboration, B. Alessandro et al., Phys. Lett. B **553**, 167 (2003)
5. NA50 Collaboration, B. Alessandro et al., Eur. Phys. J. C **33**, 31 (2004)
6. NA50 Collaboration, B. Alessandro et al., CERN-PH-EP/2006-018, accepted for publication in Eur. Phys. J. C
7. F. Karsch, Eur. Phys. J. C **43**, 35 (2005)

8. W.M. Alberico, A. Beraudo, A. De Pace, A. Molinari, Phys. Rev. D **72**, 114 011 (2005)
9. NA38 Collaboration, M.C. Abreu et al., Phys. Lett. B **466**, 408 (1999)
10. NA50 Collaboration, H. Santos et al., J. Phys. G Nucl. Partic. **30**, 1175 (2004)
11. PHENIX Collaboration, H. Pereira da Costa et al., Proceedings of the Quark Matter 2005 Conference, Nucl. Phys. A **774**, 747 (2006)
12. NA60 Collaboration, R. Arnaldi et al., Proceedings of the Quark Matter 2005 Conference, Nucl. Phys. A **774**, 711 (2006)
13. NA50 Collaboration, M.C. Abreu et al., Phys. Lett. B **410**, 327 (1997)
14. R. Shahoyan, J/ψ and ψ' production in 450 GeV p–A interactions and its dependence on rapidity and $x_{\rm F}$, PhD Thesis, Universidade Técnica de Lisboa, IST, April 2001, available at http://na50.web.cern.ch/NA50/theses.html
15. C. Lourenço, J/ψ, ψ' and dimuon production in p–A and S–U collisions at 200 GeV/nucleon, PhD Thesis, Universidade Técnica de Lisboa, IST, January 1995, available at http://www.cern.ch/NA38/theses/carlosl.ps.gz
16. H. Santos, J/ψ and ψ' production in Pb–Pb collisions at 158 GeV/nucleon, PhD Thesis, Universidade Técnica de Lisboa, IST, October 2004, available at http://na50.web.cern.ch/NA50/theses.html
17. T. Sjöstrand, Comput. Phys. Commun. **82**, 74 (1994)
18. M. Gluck, E. Reya, A. Vogt, Z. Phys. C **67**, 433 (1995)
19. L. Capelli, Étude des dimuons de la région des masses intermediaires produits dans les collisions d'ions lourds auprès du SPS du CERN, PhD Thesis, Université Claude Bernard-Lyon 1, Mars 2001, available at http://na50.web.cern.ch/NA50/theses.html
20. MINUIT – Function minimization and error analysis, reference manual, version 96.03, Computing and Networks Division – CERN
21. Particle Data Group, S. Eidelman et al., Phys. Lett. B **592**, 1 (2004)
22. CTEQ Collaboration, H.L. Lai et al., Phys. Rev. D **55**, 1280 (1997)
23. M. Gluck, E. Reya, A. Vogt, Eur. Phys. J. C **5**, 461 (1998)
24. G. Borges, J/ψ and ψ' production in p–A collisions at 400 GeV and S–U interactions at 200 GeV/nucleon, PhD Thesis, Universidade Técnica de Lisboa, IST, November 2005, available at http://na50.web.cern.ch/NA50/theses.html
25. NA50 Collaboration, G. Borges et al., Eur. Phys. J. C **43**, 161 (2005)
26. R.J. Glauber, Lectures in Theoretical Physiscs, ed. by W.E. Brittin, L.G. Dunham (Interscience, New York, 1959), Vol. 1, p. 315
27. H. De Vries et al., Atom. Data Nucl. Data **36**, 495 (1987)
28. A. Trzcinska et al., Phys. Rev. Lett. **87**, 082 501-1 (2001)
29. A. Capella et al., Phys. Lett. B **206**, 472 (1988)
30. C. Gerschel, J. Hufner, Phys. Lett. B **207**, 253 (1988)
31. D. Kharzeev, C. Lourenço, M. Nardi, H. Satz, Z. Phys. C **74**, 307 (1997)
32. WA98 Collaboration, M.M. Aggarwal et al., Eur. Phys. J. C **18**, 651 (2001)
33. WA98 Collaboration, M.M. Aggarwal et al., Nucl. Phys. A **619**, 200c (1996)
34. J.D. Bjorken, Phys. Rev. D **27**, 140 (1983)
35. J.P. Blaizot, J.Y. Ollitrault, Phys. Rev. Lett. **77**, 1703 (1996)